Comparison Between Analytic Derivative and the Technique of Differential Contributions in Reflectarray Phase-Only Synthesis

Daniel R. Prado*, Manuel Arrebola†, Marcos R. Pino† and George Goussetis*
*Institute of Sensors, Signals and Systems, Heriot-Watt University, Edinburgh, U.K. Email: {dr38, g.goussetis}@hw.ac.uk
†Group of Signal Theory and Communications, Universidad de Oviedo, Spain. Email: {arrebola, mpino}@uniovi.es

***Abstract*—Many algorithms for the optimization of array antennas need the calculation of a gradient to minimize a cost function. Usually, the best approach is to compute analytically the derivatives, since that way computations are faster. However, sometimes the derivatives are cumbersome to obtain or they cannot be calculated, such as when directly optimizing the layout in reflectarrays for cross-polarization improvement. In those cases, derivatives are evaluated using numerical techniques such as finite differences. In this work, we present the numerical technique of differential contributions (DFC) to accelerate gradient-based algorithms when the derivatives are calculated with finite differences, achieving a complexity time scaling of the same order as the analytical derivatives. The technique is applied to a far field phase-only synthesis for reflectarray antennas using the generalized Intersection Approach, and it is compared with the analytic derivatives and the use of finite differences with the FFT. The DFC technique shows superior performance in all cases, even than the analytic derivative.**

***Index Terms*—Gradient-based algorithm, optimization, synthesis, reflectarray, array, far field, differential contributions, finite differences, generalized Intersection Approach**

I. Introduction

Radiation pattern synthesis is necessary for applications that require non-canonical beams. For instance, space applications such as Direct Broadcast Satellite (DBS) [1], where the antenna must generate a specific footprint on the Earth surface; Synthetic Aperture Radar [2], where the pattern must be much wider in one principal plane than the other; global Earth coverage [3], where an isoflux pattern providing constant flux on the Earth surface may be employed. Other applications such Local Multipoint Distribution Service [4], cross-polarization improvement [5], etc., also require non-canonical beams. In addition, near field applications such as multi-focus [6] or Compact Antenna Test Range [7] also benefit from optimizing the radiated field.

A usual approach to perform array antenna synthesis is to employ a local optimizer, which usually requires the computation of the gradient of the cost function to minimize [5]–[9]. When possible, the best strategy is to analytically obtain the derivatives so computations are faster than using numerical methods. However, there might be situations in which this is not possible, either because the derivatives are cumbersome to obtain, or because they are not available, such as when performing the direct optimization of the layout for cross-polarization improvement [5], [10]. In those cases, finite differences must be use, which slows the computation of the gradient with regard to the use of the analytical derivative.

In this work, we propose the technique of differential contributions (DFC) [11] to accelerate the computation of the gradient in local search algorithm for array antenna synthesis when using finite differences. It is based on two principles. First, thanks to the linearity of Maxwell's equations, there is a linear relation between the tangential field at the aperture and the radiated field. In addition, by analysing each array element assuming local periodicity, the modification of one element, does not affect the others. These assumptions allow to consider the differential contribution to the radiated field of only one element when computing each derivative of the gradient, effectively accelerating its computations when using finite differences. This technique is implemented in generalized Intersection Approach for a far-field phase-only synthesis (POS) and compared with the performance when using finite differences with the Fast Fourier Transform (FFT), and the analytical derivative. The proposed technique consistently provides faster results, even when compared to the analytical derivative, while the achieving a high accuracy in the computation of the gradient.

II. Optimization Algorithm

A. Generalized Intersection Approach

The chosen algorithm is the generalized Intersection Approach (IA) [12] particularized for POS in [9]. It is an iterative algorithm that performs two operations on the radiated field at each iteration:

$$\vec{E}_{i+1} = \mathscr{B}\left[\mathscr{F}\left(\vec{E}_i\right)\right], \tag{1}$$

where $\mathscr{F}$ is the forward projector, which computes the radiated field and then trims it according to some specifications given in the form of lower and upper masks; and $\mathscr{B}$ is the backward projector, which minimizes the distance between the current radiated field by the reflectarray and the field trimmed by the forward projector that complies with the specifications [10].

For the present case, a far field synthesis will be performed, and the generalized IA works with the squared field amplitude, or equivalently, the gain. We consider a reflectarray antenna as a particular case of a phased-array, comprised of N elements and whose radiated field is computed at M points in space.

Assuming that S variables are optimized, and denoting with $G_t(u,v)$ the trimmed gain by the forward projector, and with $G(u,v)$ the current gain pattern radiated by the reflectarray, the cost function which is minimized by the backward projector is [10]:

$$F(\vec{r}) = \sum_{m=1}^{M} \left\{ C(\vec{r}) \left[G_t(\vec{r}) - G\left(\vec{r};\bar{\xi}\right) \right] \right\}^2, \tag{2}$$

where $\vec{r} \in \{\vec{r}_1,\ldots,\vec{r}_t,\ldots,\vec{r}_M\}$ is an observation point where the far field is computed, with $\vec{r}_t = (u,v)_t$, $u = \sin\theta\cos\varphi$, $v = \sin\theta\sin\varphi$; $C(\vec{r})$ is a weighting function and $\bar{\xi} = (\xi_1,\ldots,\xi_i,\ldots,\xi_S)$ is a vector of S optimization variables, which for the POS will be the phase-shift introduced by the reflectarray elements. The cost function in (2) is minimized by the Levenberg-Marquardt Algorithm (LMA) [13], which requires the computation of the Jacobian matrix formed with the derivatives of the residuals:

$$R\left(\vec{r};\bar{\xi}\right) = C(\vec{r})\left(G_t(\vec{r}) - G\left(\vec{r};\bar{\xi}\right)\right). \tag{3}$$

Since we consider S optimizing variables, the LMA will require to compute S derivatives of (3).

B. Analytical Derivative

From here on, we drop the dependence on $\vec{r}$ to alleviate notation and to focus only on the optimization variables $\bar{\xi}$. Since for POS the optimization variables are the phase-shifts introduced by the reflectarray elements, there is an easy way to obtain the derivative analytically. For the computation of the Jacobian matrix (gradient), we need to obtain the following derivative:

$$R'\left(\bar{\xi}\right) = \frac{\partial R\left(\bar{\xi}\right)}{\partial \xi_i} = \frac{\partial\left[C\cdot\left(G_t - G(\bar{\xi})\right)\right]}{\partial \xi_i}. \tag{4}$$

The apostrophe indicates a partial derivative with respect to variable ξ_i. In addition, the gain is proportional to the squared far field amplitude:

$$G\left(\bar{\xi}\right) = \frac{2\pi}{\eta_0 P_t}\left|E_{\text{ff}}\left(\bar{\xi}\right)\right|^2, \tag{5}$$

where $\eta_0 = \mu_0 c$ is the intrinsic impedance of vacuum and P_t the power radiated by the feed. Thus, we can rewrite the residual in (3) as:

$$R\left(\bar{\xi}\right) = C_1 - C_2\left|E_{\text{ff}}\left(\bar{\xi}\right)\right|^2, \tag{6}$$

where:

$$C_1 = CG_t \quad ; \quad C_2 = C\frac{2\pi}{\eta_0 P_t}. \tag{7}$$

Taking into account that $E_{\text{ff}}\left(\bar{\xi}\right)$ is complex, and it can be written as the sum of its real and imaginary parts:

$$E_{\text{ff}}\left(\bar{\xi}\right) = E_{\text{ff,R}}\left(\bar{\xi}\right) + jE_{\text{ff,I}}\left(\bar{\xi}\right), \tag{8}$$

using the chain rule, it follows:

$$R'\left(\bar{\xi}\right) = -2C_2\left[E_{\text{ff,R}}\left(\bar{\xi}\right)E'_{\text{ff,R}}\left(\bar{\xi}\right) + E_{\text{ff,I}}\left(\bar{\xi}\right)E'_{\text{ff,I}}\left(\bar{\xi}\right)\right]. \tag{9}$$

For the far field, we consider the copolar component in two linear polarizations [14], which are:

$$E^X_{\text{ff}}\left(\bar{\xi}\right) = E^X_{\text{CP}}\left(\bar{\xi}\right) = \cos\varphi E^X_\theta\left(\bar{\xi}\right) - \sin\varphi E^X_\varphi\left(\bar{\xi}\right), \tag{10a}$$

$$E^Y_{\text{ff}}\left(\bar{\xi}\right) = E^Y_{\text{CP}}\left(\bar{\xi}\right) = \sin\varphi E^Y_\theta\left(\bar{\xi}\right) + \cos\varphi E^Y_\varphi\left(\bar{\xi}\right), \tag{10b}$$

which are again complex numbers and need to be expressed in their real and imaginary parts. In addition, since the POS is done independently for each linear polarization, we will focus on polarization X. The steps for polarization Y will be identical. Thanks to the linearity of the differential operator, (9) can be written as:

$$\begin{aligned} R'\left(\bar{\xi}\right) = -2C_2\Big[&E^X_{\text{CP,R}}\left(\bar{\xi}\right)\left(\cos\varphi E'_{\theta,R}\left(\bar{\xi}\right) - \sin\varphi E'_{\varphi,R}\left(\bar{\xi}\right)\right) \\ &+ E^X_{\text{CP,I}}\left(\bar{\xi}\right)\left(\cos\varphi E'_{\theta,I}\left(\bar{\xi}\right) - \sin\varphi E'_{\varphi,I}\left(\bar{\xi}\right)\right)\Big] \end{aligned} \tag{11}$$

For POS, the far field in spherical coordinates for polarization X are [9]:

$$\begin{aligned} E^X_\theta\left(\bar{\xi}\right) = A\Big[&P^X_x\left(\bar{\xi}\right)\cos\varphi - \eta_0\cos\theta\left(Q^X_x\left(\bar{\xi}\right)\sin\varphi - \right. \\ &\left. Q^X_y\left(\bar{\xi}\right)\cos\varphi\right)\Big], \end{aligned} \tag{12a}$$

$$\begin{aligned} E^X_\varphi\left(\bar{\xi}\right) = -A\Big[&P^X_x\left(\bar{\xi}\right)\sin\varphi\cos\theta + \eta_0\left(Q^X_x\left(\bar{\xi}\right)\cos\varphi + \right. \\ &\left. Q^X_y\left(\bar{\xi}\right)\sin\varphi\right)\Big], \end{aligned} \tag{12b}$$

where A is:

$$A = \frac{jk_0\exp\left(-jk_0 r\right)}{4\pi r}. \tag{13}$$

At this point, A is a complex number, as well as the spectrum functions P and Q. Since we need the real and imaginary parts of (12), it seems that we need to consider the multiplication of A with P and Q. However, A is a common factor to all equations and does not depend on the optimization variables. Thus, we can extract it from (12) and add it to C_2 in (9) so the following operations are simplified. With that, the real and imaginary parts of E_θ are:

$$\begin{aligned} E^X_{\theta,R}\left(\bar{\xi}\right) = \cos\varphi P^X_{x,R}\left(\bar{\xi}\right) - \eta_0\cos\theta\sin\varphi Q^X_{x,R}\left(\bar{\xi}\right) + \\ \eta_0\cos\theta\cos\varphi Q^X_{y,R}\left(\bar{\xi}\right), \end{aligned} \tag{14a}$$

$$\begin{aligned} E^X_{\theta,I}\left(\bar{\xi}\right) = \cos\varphi P^X_{x,I}\left(\bar{\xi}\right) - \eta_0\cos\theta\sin\varphi Q^X_{x,I}\left(\bar{\xi}\right) + \\ \eta_0\cos\theta\cos\varphi Q^X_{y,I}\left(\bar{\xi}\right). \end{aligned} \tag{14b}$$

And similarly for E^X_φ.

For the computation of the derivatives of the real and imaginary parts of E^X_θ and E^X_φ, we need to compute the derivatives of the real and imaginary parts of the spectrum functions P and Q, by virtue of the linear property of the differential operator. For instance, a generic spectrum function P takes the form:

$$P\left(\bar{\xi}\right) = K\sum_{i=1}^{N}\exp\left(j\xi_i\right)E_{\text{inc},i}\exp\left(jk_0(ux_i + vy_i)\right), \tag{15}$$

where $K \in \mathbb{R}$ is the amplitude of the element pattern [15], $E_{\text{inc},i}$ is the complex incident field on reflectarray element i

and ξ_i the phase-shift introduced by that element, which is the optimization variable for the POS. After extracting the real and imaginary parts of (15), we have:

$$P_R\left(\bar{\xi}\right) = K\sum_{i=1}^{N}\Big[\cos\xi_i E_{\text{inc},i,R}\cos k_i - \sin\xi_i E_{\text{inc},i,I}\cos k_i - \cos\xi_i E_{\text{inc},i.I}\sin k_i - \sin\xi_i E_{\text{inc},i,R}\sin k_i\Big], \tag{16a}$$

$$P_I\left(\bar{\xi}\right) = K\sum_{i=1}^{N}\Big[\cos\xi_i E_{\text{inc},i,R}\sin k_i - \sin\xi_i E_{\text{inc},i,I}\sin k_i + \cos\xi_i E_{\text{inc},i,I}\cos k_i + \sin\xi_i E_{\text{inc},i,R}\cos k_i\Big], \tag{16b}$$

where $k_i = k_0(ux_i + vy_i)$. Thus, the derivative for any element $i = p$ is:

$$P'_R\left(\bar{\xi}\right) = -K\Big[\sin\xi_p E_{\text{inc},p,R}\cos k_p + \cos\xi_p E_{\text{inc},p,I}\cos k_p - \sin\xi_p E_{\text{inc},p,I}\sin k_p + \cos\xi_p E_{\text{inc},p,R}\sin k_p\Big], \tag{17a}$$

$$P'_I\left(\bar{\xi}\right) = -K\Big[\sin\xi_p E_{\text{inc},p,R}\sin k_p + \cos\xi_p E_{\text{inc},p,I}\sin k_p + \sin\xi_p E_{\text{inc},p,I}\cos k_p - \cos\xi_p E_{\text{inc},p,R}\cos k_p\Big]. \tag{17b}$$

The derivatives in (17) can be used for the four cases $P^{X/Y}_{x/y}$ by simply using the adequate incidence field. For instance, the spectrum function P^X_y would need the field $E^X_{\text{inc},y}$. For the spectrum functions Q, which use the magnetic field [9], a similar process is carried out, yielding similar derivatives as in (17). Finally, as it can be seen, the computation of the derivative only considers the contribution of the element depending on variable ξ_i, and thus the time cost of computing one derivative analytically is $\mathcal{O}(M)$.

C. Gradient Computation with Differential Contributions

An alternative numerical method for the computation of the gradient is the Differential Contributions (DFC) technique. It accelerates the computation of the gradient when it is evaluated using finite differences, achieving a time cost similar to that of the analytic derivative. The derivative in (4) may be expressed using finite differences, for instance the backward lateral difference [16]:

$$\frac{\partial R(\bar{\xi})}{\partial \xi_i} = \frac{R(\bar{\xi}) - R(\bar{\xi} - h\hat{e}_i)}{h} + \mathcal{O}(h), \tag{18}$$

where h is a small positive scalar [13] and $\hat{e}_i$ the ith unit vector.

For the computation of the derivative by means of (18), the residual $R(\bar{\xi})$ depends on the far field $E_{\text{ff}}(\bar{\xi})$ and it is common to all S derivatives of the Jacobian matrix, so it only needs to be computed once. On the other hand, $R(\bar{\xi} - h\hat{e}_i)$ depends on $E_{\text{ff}}(\bar{\xi} - h\hat{e}_i)$, and is computed for each derivative. In addition, the perturbed field $E_{\text{ff}}(\bar{\xi} - h\hat{e}_i)$ may be computed with the differential contribution:

$$E_{\text{ff}}(\bar{\xi} - h\hat{e}_i) = E_{\text{ff}}(\bar{\xi}) + \Delta E_{\text{ff}}(\xi_i), \tag{19}$$

where $\Delta E_{\text{ff}}(\xi_i)$ is the differential contribution to the far field produced by the element depending on variable i:

$$\Delta E_{\text{ff}}(\xi_i) = E_{\text{ff}}(\xi_i - h) - E_{\text{ff}}(\xi_i). \tag{20}$$

This is possible since the far field may be computed as contribution of the field radiated by of all the elements of the reflectarray, as in (15).

Since the Maxwell's equations are linear, there exits a linear relation between the tangential field at the aperture and the radiated field. If we denote by $E_{\text{ref},k}(\xi_i) = \exp(j\xi_i)E_{\text{inc},k}$ the reflected tangential field of element k with $k = 1,\ldots,N$ and depending on variable ξ_i, (20) can be expressed writing the far field as a function of the tangential field:

$$\Delta E_{\text{ff}}(\xi_i) = E_{\text{ff}}(E_{\text{ref},k}(\xi_i - h)) - E_{\text{ff}}(E_{\text{ref},k}(\xi_i)). \tag{21}$$

Since the radiated field is linear with respect to the tangential field it follows:

$$\Delta E_{\text{ff}}(\xi_i) = E_{\text{ff}}(\Delta E_{\text{ref},k}(\xi_i)), \tag{22}$$

where:

$$\Delta E_{\text{ref},k}(\xi_i) = E_{\text{ref},k}(\xi_i - h) - E_{\text{ref},k}(\xi_i). \tag{23}$$

Thus, (22) indicates that to compute one derivative, only the differential contribution of one element is necessary, i.e., the element which depends on variable ξ_i. In practise, this means that, starting from the tangential field, the time cost of computing the far field is reduced from $\mathcal{O}(M\log M)$ when using the FFT to $\mathcal{O}(M)$ using the DFC technique. This time cost is the same as for the analytic derivative.

D. Computational Results

The DFC technique has been compared with other techniques for the computation of the Jacobian matrix: finites differences using the FFT for the calculation of the far field, and the analytic derivative obtained in Section II.B. Simulations were performed in a workstation with an Intel Xeon E5-2630 v4 CPU at 2.2 GHz with 10 cores and 20 threads. In addition, the computation of the Jacobian is parallelized, computing one derivative (corresponding to a Jacobian column) per available thread. Finally, the grid in which the far field is obtained has 512×512 points.

In Fig. 1 the measured computing time is shown when optimizing a reflectarray with different number of elements, or equivalently, reflectarrays of different size. From the results shown in Fig. 1, the DFC technique is faster than the FFT and even the analytic derivative, which a priori would seem to be the fastest solution. In the present case, both the DFC technique and analytic derivative have a time cost of $\mathcal{O}(SM)$ for the computation of the gradient (Jacobian matrix), where S is the number of optimization variables and M the number of points where the far field is computed. However, the analytic derivative requires more calculations in the loop that sweeps the M points, resulting in the DFC technique being around 30% faster than the analytic derivative, and 56.9% and 94.2% faster than the FFT and NUFFT, respectively.

III. Application to the Synthesis of a Large Reflectarray for Direct Broadcast Satellite

A. Antenna Specifications

In this section, the DFC technique is applied to the synthesis of a very large reflectarray for a Direct Broadcast

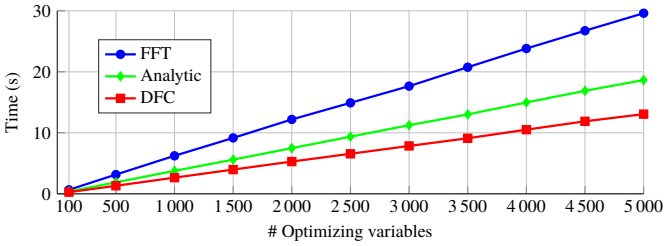

Fig. 1. Measured computing time of the Jacobian matrix computation with the FFT, Diferential Contributions (DFC) and analytic derivative for different number of optimization variables using a UV grid of 512×512 points and computations parallelized with 20 threads.

Satellite mission with European coverage [10]. The considered reflectarray is rectangular and comprised of 5 180 elements arranged in a periodic grid of 74×70. For the feed, an ideal model based on a $\cos^q \theta$ function is employed [17], with $q = 23$ generating an illumination taper of -17.9 dB, and is placed at coordinates $(-358, 0, 1070)$ mm with respect to the center of the reflectarray. The periodicity of the unit cell is $14 \times 14\,\text{mm}^2$ and the working frequency is 11.85 GHz. Finally, the reflectarray is placed in a satellite in geostationary orbit at 10° E longitude.

B. Results

Two different syntheses were carried out, the first using the analytic derivative, and the second using the DFC technique. The phase distributions obtained with each technique were compared and Fig. 2 shows the difference for polarization X. As it can be seen, the largest differences are produced at the edges, which present the lowest illumination from the feed and thus will affect less to the radiation pattern. For Fig. 2, the mean absolute deviation is 1.6°. In addition, the deviation was also computed after the first iteration of the algorithm, showing a mean absolute deviation of only 0.0034° ($5.9 \cdot 10^{-5}$ rad). Taking into account the total number of reflectarray elements, it is consistent with the expected error of using finite differences, which for a lateral difference using real numbers of 8 bytes is of the order of $\mathcal{O}(10^{-8})$ [16]. Fig. 3 shows the obtained copolar pattern for polarization X using both methods. The differences due to the phase distribution not being the same are negligible. Similar results were obtained for polarization Y regarding the phase distributions and radiation pattern.

Finally, it took the generalized Intersection Approach 149 iterations to obtain the results of Fig. 3, performing three iterations of the LMA per iteration of the IA. Thus, the Jacobian matrix was evaluated a total of 447 times. Moreover, the synthesis was carried out in several stages, increasing the number of variables at each stage to minimize the local minima and improve convergence [12]. With the DFC technique, 2 875 seconds (47.9 minutes) were employed computing the gradient. If the FFT were employed for the computation, it would have taken 6 540 seconds (109 minutes) using data from Fig. 1, which supposes a speed up of approximately 56%. For the analytic derivative, the speed up was about 30% (from 4 086 seconds).

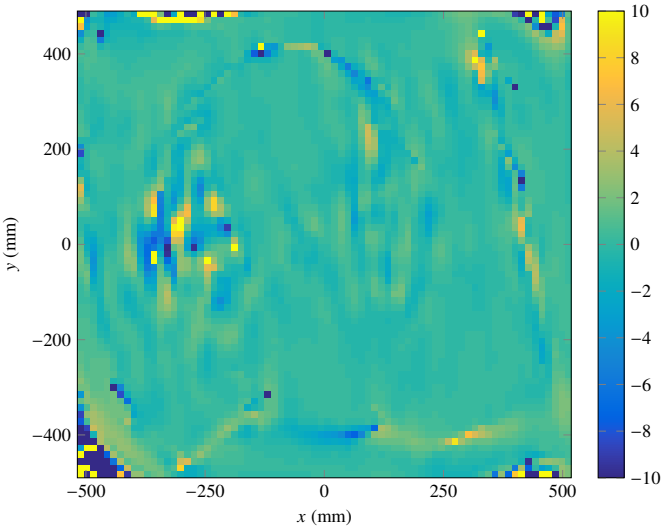

Fig. 2. Phase difference in degrees (°) between the syntheses using the analytical derivative and the DFC technique for the computation of the Jacobian matrix for polarization X.

IV. Conclusion

In this work, a technique for the acceleration of the gradient computation for reflectarray synthesis has been presented. It is based on differential contribution (DFC) to the radiated field, for which only the contribution of a single element is considered. This way, the far field synthesis is sped up. This technique has been implemented for a Phase-Only Synthesis (POS) using the generalized Intersection Approach, where the analytic derivative is available. A computing time study comparing the DFC with other techniques for the computation of the gradient was presented, including the analytic derivative and the use of the FFT for the computation of the far field using finite differences. The new technique is the fastest for the computation of the gradient, even when compared to the analytic derivative, since it has fewer operations for the computation of the gradient. Finally, the technique was employed for the synthesis of a very large reflectarray for a Direct Broadcast Satellite mission with European coverage. The results were compared with those of another synthesis using the analytic derivative and the differences between the two were negligible, while the DFC provides a computation of the gradient around 30% faster.

Acknowledgment

This work was supported in part by the European Space Agency (ESA) under contract ESTEC/AO/1-7064/12/NL/MH; by the Ministerio de Ciencia, Innovación y Universidades under project TEC2017-86619-R (ARTEINE); by the Ministerio de Economía, Industria y Competitividad under project TEC2016-75103-C2-1-R (MYRADA); and by the Gobierno del Principado de Asturias through Programa “Clarín” de

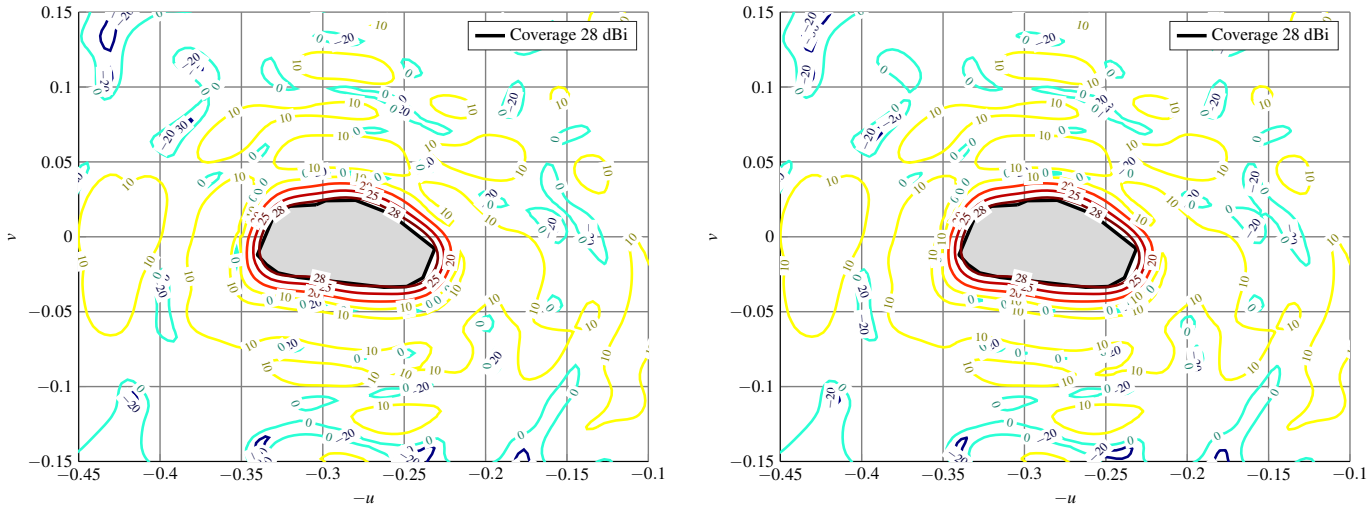

(a) (b)

Fig. 3. Copolar pattern for polarization X in gain (dBi) of the synthesized European coverage obtained using (a) analyticla derivatives and (b) the differentical contributions technique.

Ayudas Postdoctorales / Marie Courie-Cofund under project ACA17-09.

REFERENCES

[1] J. A. Encinar, R. Florencio, M. Arrebola, M. A. Salas-Natera, M. Barba, J. E. Page, R. R. Boix, and G. Toso, "Dual-polarization reflectarray in Ku-band based on two layers of dipole arrays for a transmit-receive satellite antenna with South American coverage," *Int. J. Microw. Wirel. Technol.*, vol. 10, no. 2, pp. 149–159, 2018.

[2] C. Tienda, M. Younis, P. López-Dekker, and P. Laskowski, "Ka-band reflectarray antenna system for SAR applications," in *The 8th European Conference on Antennas and Propagation (EUCAP)*, The Hague, The Netherlands, Apr. 6–11, 2014, pp. 1603–1606.

[3] D. R. Prado, A. Campa, M. Arrebola, M. R. Pino, J. A. Encinar, and F. Las-Heras, "Design, manufacture and measurement of a low-cost reflectarray for global Earth coverage," *IEEE Antennas Wireless Propag. Lett.*, vol. 15, pp. 1418–1421, 2016.

[4] M. Arrebola, J. A. Encinar, and M. Barba, "Multifed printed reflectarray with three simultaneous shaped beams for LMDS central station antenna," *IEEE Trans. Antennas Propag.*, vol. 56, no. 6, pp. 1518–1527, Jun. 2008.

[5] M. Zhou, S. B. Sørensen, O. S. Kim, E. Jørgensen, P. Meincke, and O. Breinbjerg, "Direct optimization of printed reflectarrays for contoured beam satellite antenna applications," *IEEE Trans. Antennas Propag.*, vol. 61, no. 4, pp. 1995–2004, Apr. 2013.

[6] J. Álvarez, R. G. Ayestarán, G. León, L. F. Herrán, A. Arboleya, J. A. López-Fernández, and F. Las-Heras, "Near field multifocusing on antenna arrays via non-convex optimisation," *IET Microw. Antennas Propag.*, vol. 8, no. 10, pp. 754–764, Jul. 2014.

[7] D. R. Prado, A. F. Vaquero, M. Arrebola, M. R. Pino, and F. Las-Heras, "General near field synthesis of reflectarray antennas for their use as probes in CATR," *Progr. Electromagn. Res.*, vol. 160, pp. 9–17, Oct. 2017.

[8] T. H. Ismail, D. I. Abu-Al-Nadi, and M. J. Mismar, "Phase-only control for antenna pattern synthesis of linear arrays using the Levenberg-Marquardt algorithm," *Electromagnetics*, vol. 24, no. 7, pp. 555–564, 2004.

[9] D. R. Prado, M. Arrebola, M. R. Pino, and F. Las-Heras, "Improved reflectarray phase-only synthesis using the generalized intersection approach with dielectric frame and first principle of equivalence," *Int. J. Antennas Propag.*, vol. 2017, pp. 1–11, May 2017.

[10] D. R. Prado, M. Arrebola, M. R. Pino, R. Florencio, R. R. Boix, J. A. Encinar, and F. Las-Heras, "Efficient crosspolar optimization of shaped-beam dual-polarized reflectarrays using full-wave analysis for the antenna element characterization," *IEEE Trans. Antennas Propag.*, vol. 65, no. 2, pp. 623–635, Feb. 2017.

[11] D. R. Prado, A. F. Vaquero, M. Arrebola, M. R. Pino, and F. Las-Heras, "Acceleration of gradient-based algorithms for array antenna synthesis with far field or near field constraints," *IEEE Trans. Antennas Propag.*, 2018, in press (available in early access).

[12] O. M. Bucci, G. D'Elia, G. Mazzarella, and G. Panariello, "Antenna pattern synthesis: a new general approach," *Proc. IEEE*, vol. 82, no. 3, pp. 358–371, Mar. 1994.

[13] D. R. Prado, J. Álvarez, M. Arrebola, M. R. Pino, R. G. Ayestarán, and F. Las-Heras, "Efficient, accurate and scalable reflectarray phase-only synthesis based on the Levenberg-Marquardt algorithm," *Appl. Comp. Electro. Society Journal*, vol. 30, no. 12, pp. 1246–1255, Dec. 2015.

[14] D. R. Prado, M. Arrebola, M. R. Pino, and F. Las-Heras, "Complex reflection coefficient synthesis applied to dual-polarized reflectarrays with cross-polar requirements," *IEEE Trans. Antennas Propag.*, vol. 63, no. 9, pp. 3897–3907, Sep. 2015.

[15] ——, "An efficient calculation of the far field radiated by non-uniformly sampled planar fields complying Nyquist theorem," *IEEE Trans. Antennas Propag.*, vol. 63, no. 2, pp. 862–865, Feb. 2015.

[16] J. Nocedal and S. J. Wright, *Numerical Optimization*, 2nd ed. New York, NY, USA: Springer, 2006.

[17] Y.-T. Lo and S.-W. Lee, Eds., *Antenna Handbook Vol. 1*. New York, NY, USA: Van Nostrand Reinhold, 1993, ch. 1, pp. 28–29.